Werner Fuchs, Jan Hofmann (Hg.)

BEFESTIGUNGSTECHNIK BEWEHRUNGSTECHNIK UND . . . II

Rolf Eligehausen zum 70. Geburtstag

2012

ibidem-Verlag
Stuttgart

WAKE-UP CALL FOR CREEP, MYTH ABOUT SIZE EFFECT AND BLACK HOLES IN SAFETY: WHAT TO IMPROVE IN *fib* MODEL CODE DRAFT*)

Zdeněk P. Bažant, Qiang Yu, Mija Hubler, Vladimír Křístek and Zdeněk Bittnar
Department of Civil and Environmental Engineering, Northwestern University Evanston

Abstract

Although the 2010 Draft of *fib* Model Code is overall an excellent document, it has some weaknesses which could, and should, be corrected. One is the material model for creep and shrinkage prediction, which not only is theoretically obsolete but also is indefensible in view of the wake-up call provided by recently collected long-term deflections of 56 bridges. The second is a size effect formulation for shear strength whose justification is tantamount to a myth rather than reason. The third consists of the probability distribution of structural strength for failures occurring at macro-crack initiation. The distribution tail that matters, in the probability range of 10^{-6}, is directly unobservable, just like a black hole. But indirect evidence from the size effect indicates that the distribution transits from Gaussian to Weibulian as the structure size increases. This transition may have a major effect on the safety factor. Moreover, dubious uses of the lognormal distribution and another black hole in the covert safety factors implied in the design formulas render a meaningful calculation of failure probability impossible. Some remedies are offered.

*This paper is an authorized republication of the paper with the same title and the same authors, presented as the Topic 3 Keynote Lecture at the *fib* Symposium in Prague in June 2011 and published in the proceedings volume entitled "Concrete Engineering for Excellence and Efficiency" (ISBN 978-87158-26-7), pp. 731--746.

1. Wake-up call from excessive long-term deflections of 56 bridges

In two recent studies [1, 2], the data on the collapse in 1996 of the Koror-Babeldaob (KB) Bridge in Palau, released in 2008, were analyzed. Built in 1977, this prestressed segmentally erected box girder had the world-record span of 241 m. Within 18 years, it deflected by 1.61 m, compared to the design camber, and the average prestress loss in the tendons (bonded bars) was measured as 49% (Fig. 1). Remedial prestressing undertaken in 1996 caused, with a 3-month delay, a sudden collapse (with fatalities). This spectacular collapse was what triggered attention to the earlier huge creep deflections and to their similarities with other bridges.

A resolution of the 3rd Structural Engineers' World Congress in 2007 (proposed by Bažant) labeled an engineer's consent to the sealing of technical data from legal litigation of structural collapses and damages as a violation of engineering ethics [1]. Two months later (in 2008), the technical data from the collapse investigation and litigation were released to Northwestern University (by Gary Klein of Wiss, Janney and Elstner, Highland Park, Illinois); also [3, 4, 5, 6, 7]. This made possible a three-dimensional (3D) finite-element step-by-step creep analysis, taking into account the effects of cracking, segmental erection, sequential prestressing, concrete aging, age differences, shear lags in slabs and walls, non-uniform shrinkage, nonuniform drying creep properties, temperature and gradual stress relaxation in prestressing steel.

The results have shown that the excessive deflections and prestress loss can be explained and closely matched if the theoretically based model B3 [8, 9] (which became a 1995 RILEM Recommendation [8]) is used to characterize the creep and shrinkage properties, provided that this model is recalibrated by the 30-year laboratory creep tests of Brooks [10]; see the Set 2 curves in Fig. 1. Models other than RILEM-B3, which include the current ACI-209, CEB-fib, GL and JSCE models for creep and shrinkage prediction [11, 12, 13, 14, 15, 16, 17, 18], have a form that does not allow recalibration by laboratory data. The same finite element program for 3D creep analysis was also run for these models (Fig. 1) as well as for model RILEM-B3 as originally calibrated by a worldwide laboratory database (see Set 1 curves in Fig. 1). The 18-year mid-span deflections computed from the CEB-fib, ACI-209, and GL models and the non-recalibrated model RILEM-B3 (Set 1) were, respectively, 34%, 31%, 43% and 57% of the measured deflection, and the computed 18-year prestress losses were 48%, 44%, 54% and 80% of the mean measured loss.

Through the courtesy of Yasumitsu Watanabe, chief engineer of Shimizu Co., Tokyo, detailed data have subsequently been received on four of the excessively deflecting segmental bridges of that company. Their analysis [1, 2] led to the same conclusions, which were as follows:

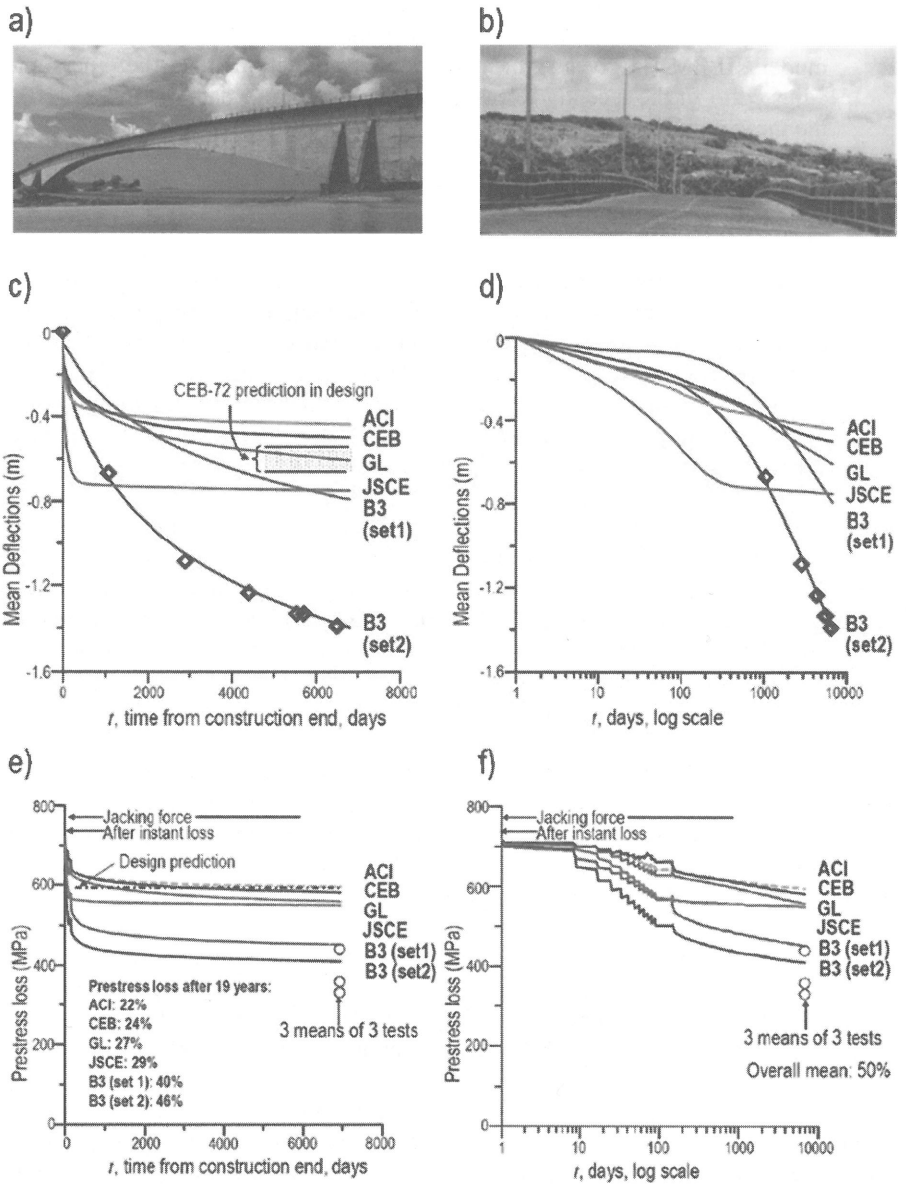

Figure 1. a,b) Creep sag of 1.61 m at mid-span of KB Bridge in Palau in 1996; b) ACI authorized reprint of photo from the cover of ACI SP-194 (2000) taken by Adam Neville before retrofit. c,d) Deflections calculated by 3D finite elements using models CEB-*fib*, ACI-209, GL, JSCE and RILEM-B3 in linear (c) and logarithmic (d) time scales, compared to measurements (data points). d,e) Similar comparisons for prestress loss.

1) The main cause of error lies in the creep and shrinkage model. All of the existing creep and shrinkage prediction models are unsatisfactory. Nonetheless, model RILEM-B3 gives significantly better predictions than the others and, if adjusted to fit the recently released 30-year laboratory data of Brooks [10], fits the measurements in Palau closely [1, 2].

2) Hence, the creep specifications of *fib* [13, 14] (as well as ACI-209 [11, 12]) need to be revised.

3) Secondary contributing causes are the use of obsolete beam-type creep analysis programs, neglect of differences in shrinkage and drying creep rates in slabs of different thicknesses and different thermal exposures, disregard of nonlinear response due to cracking, gross underestimation of prestress losses, poor representation of segmental erection, of sequential prestressing and of concrete age differences and, as a minor contribution, also the cyclic creep due to traffic loads [2].

Are the excessive deflections rare? They are not. A subsequent search of various papers, company reports and society reports under the auspices of the newly founded RILEM Committee TC-MDC led to a wake-up call—see Fig. 2 documenting the deflection histories of 56 large-span bridge spans [19, 20, 21, 22, 23], most of them excessive (all are segmental box girders except for one arch, and the horizontal dashed lines show the maximum acceptable deflection, 1/800 of the span). Hard to obtain though such examples are, hundreds more probably exist.

Of course, segmental bridges that have not deflected excessively (such as the Pine Valley Creek Bridge in California built in 1975) exist, too, but appear to be a minority. Even if a poor creep model is used, the deflections can be low if one adopts various precautionary measures listed at the end of [1, 2]. Some of them, though, are costly or span-limiting and detract from esthetic slenderness.

The logarithmic time plots in Fig. 2 also give no hint of an approach to an asymptotic bound, a feature incorrectly implied by all the society recommendations except model RILEM-B3 (and its predecessors since 1978). They document that the long-term creep is a logarithmic curve (as observed on the basis of laboratory data in [24].

Why have the recommendations on creep been misleading, for decades? Aside from disregard of the theoretical basis and lax interpretation of the laboratory tests, the problem has also been the inevitable statistical bias of the world-wide laboratory database [25, 26]. In the latest and largest database, assembled at Northwestern in 2011, only 8% of creep test curves exceed 6 years, and only 5% 12 years. Also, the data readings are heavily biased for short times and ages. Even if the statistical bias is filtered by proper weighting [26], the multi-decade trend is not quite clear.

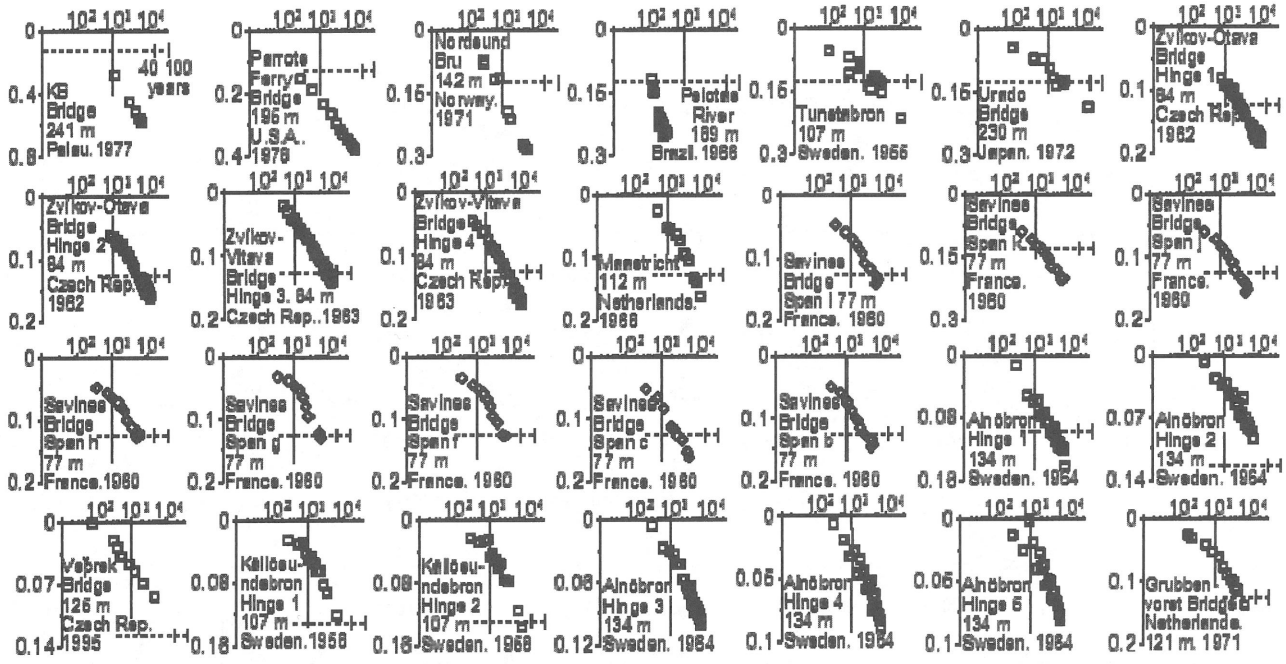

Figure 2 Deflection records on 56 prestressed segmentally built box girder bridges (as a function of time t_c after span closing, in logarithmic scale). Note that the creep compliance curves show no sign of a horizontal asymptote implied by CEB-*fib*, ACI, GL and JSCE creep models. The horizontal lines shows allowable deflection (span / 800) (for further figures, see the short paper by Bažant et al. on the CD of the present proceedings volume).

Excessive Deflections of 56 Segmental Bridge Spans [(deflection/span)% vs. time in days] ctd.

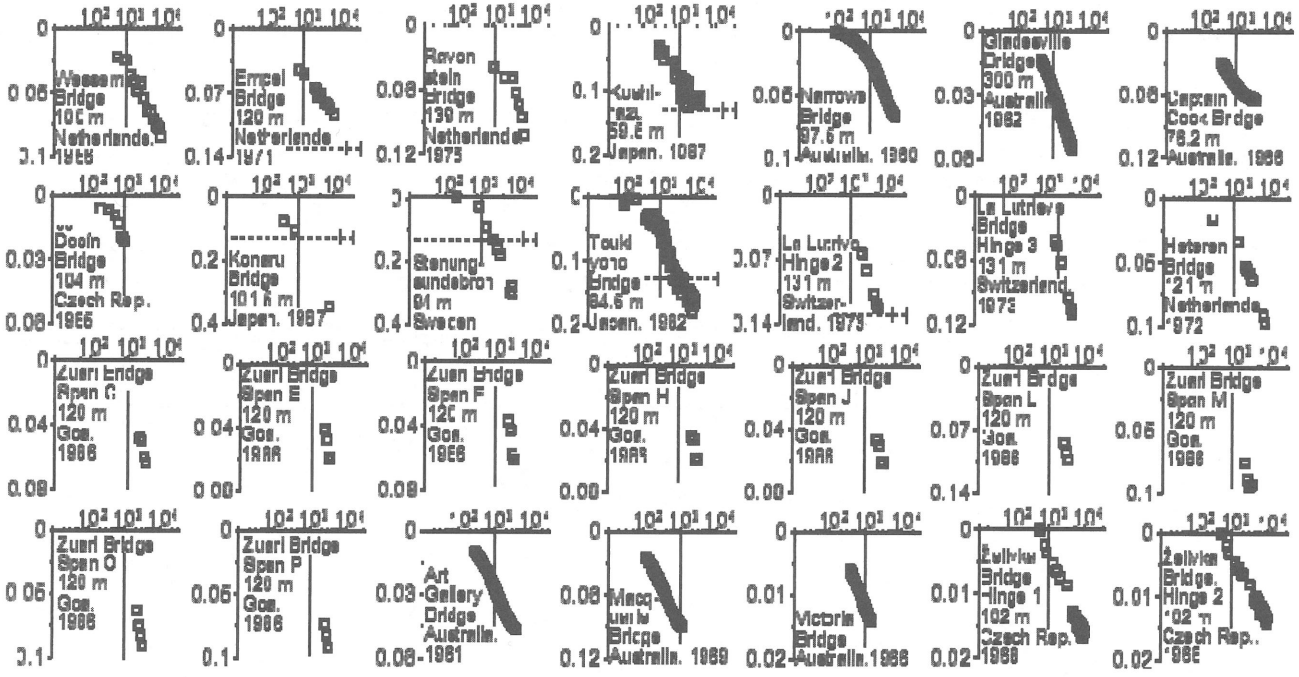

Figure 2 continued

In this light, inverse interpretation of the bridge deflection histories in Fig. 2 appears to be essential. Ideally, one should conduct statistical inverse 3D finite element creep analysis of these bridges. But it has appeared impossible to obtain data that would suffice for finite element analysis of these 56 bridges, except for 6 of them.

Nonetheless, examination of the accurate solutions of the bridge in Palau and a few others showed that, for times t > tm (where tm = tc + 1000 days, tc = span closing time), the complex effects of nonuniform drying, segmental erection, sequential prestressing, concrete age differences and changes of structural system nearly die out. By comparisons with the accurate solutions for the KB Bridge it was thus shown that the subsequent deflection $w(t)$ can be extrapolated from the measured 1000-day deflection w_{1000} with a surprisingly good accuracy by means of the formula:

$$w = w_{1000}\,[J(t, t_a) - J(t_c, t_a)] \,/\, [J(t_m, t_a) - J(t_c, t_a)] \qquad (1)$$

derived in 2010 by Bažant and verified in [27]; t_a = average age of concrete at permanent load application; $t_m = t_c + 1000$ days, t_c = time at span closing. Deflection w_{1000} at 1000 days after span closing cannot be predicted without detailed three-dimensional finite element creep analysis.

Although it turned out to be impossible to obtain the concrete strength and composition data for the 56 bridges (except 6) in Fig. 2, the average concrete properties for 36 of them (Fig. 3) could be estimated and statistical analysis conducted [27]. As a result, it was concluded that the long-time creep parameters q_3 and q_4 determined from concrete composition by the empirical formulas of model RILEM-B3 should be multiplied by correction factor $r = 1.6$. With this factor, the mean prediction of model RILEM-B3 for the terminal slopes becomes correct (Fig. 3) and the coefficient of variation of errors in the terminal slope gets greatly reduced [27].

For the creep and shrinkage model of *fib* (as well as ACI-209), similar corrections cannot be implemented because many of its aspects are theoretically incorrect. Aside from the incorrect form of Eq. 5.1-69, which implies an asymptotic bound and gives a time curve with a shape disagreeing with individual long-time creep tests (a fact that gets obfuscated when comparisons are made with the entire database), there are in Sec. 5.1.9.4 of the 2010 *fib* Model Code Draft further weak points which need to be corrected.

E.g., the effect of drying on creep (Eq. 5.1-64) should not be represented by multiplicative factor φ_{RH} on the entire creep strain [28, 29]. Like model RILEM-B3, the drying creep should rather be a term additive to the basic creep, multiplicatively scaled according to the RH and shifted horizontally on top of the basic creep curve in log-time by a distance proportional to the square of thickness $h = 2A_c/u$ [28, 9].

Another problem is that the compliance function, $J(t,t')$, of CEB-*fib* (as well as ACI-209) does not satisfy the condition of non-divergence of creep, $\partial^2 J(t,t')/\partial t \partial t' \geq 0$ [28], which causes that the principle of superposition can yield non-monotonic creep recovery curves (i.e., curves with recovery reversal). This is thermodynamically impossible according to Kelvin chain model [30].

Also, the creep should not be defined by the creep coefficient φ (Eqs. 5.1-60 to 5.1-63), for two reasons: First, it tempts engineers to use the standard elastic modulus E, whose definition and measurement is incompatible with the way the initial deformation (compliance) was measured. This typically causes an error that can be precluded by specifying the compliance function from which the creep coefficient can be calculated as $\varphi = E(t_0)J(t,t_0) - 1$. Second, the use of the conventional short-time modulus (rather than the asymptotic modulus in model RILEM-B3) forces the exponent in Eq. 5.1-69 to be too high, namely 0.3 (for short-time creep it should be about 0.1).

The alleged asymptotic bound of *fib* creep formula is approached within 98% only after 70 years. The bound was much lower for the early models of Whitney, Glanville, Ross, Dischinger, Ulickii and Arutyunyan in the 1940s and 50s [28], and was approached closely in about 3 years. Accumulation of data over the years led to a gradual increase of the bound (a historical phenomenon that may be regarded as "creep inflation"). The engineers should finally abandon wishful thinking and admit that there is no evidence of a bound.

The simplest remedy for *fib* would be to replace the creep formulation with model RILEM-B3 [8, 9]. A still better remedy would be the improved model B3.1 under development in the Northwestern Infrastructure Technology Institute and in RILEM TC-MDC.

A problem related to creep is that the steel relaxation in prestressing tendons is generally defined only for a constant strain in steel. Analysis of the KB Bridge in Palau showed that the strain in steel can change by as much as 30% during lifetime, which has a significant effect on the stress relaxation in steel as well as prestress losses. An incremental viscoplastic model for prestressing steel, which is easy to use in time steps of finite element creep analysis, has been developed [31] and should be introduced into the code.

Extrapolated Deflections of 36 Bridges [(deflection/span)% vs. time in days]

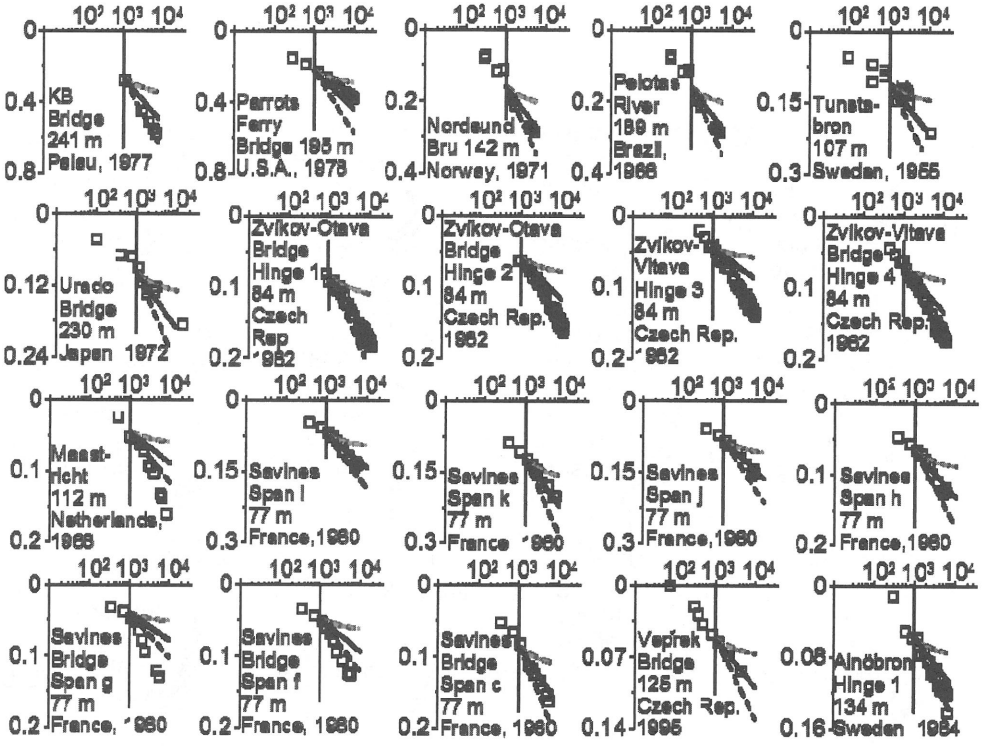

Figure 3 Extrapolations $w = C[J(t, t_a) - J(t_c, t_a)]$ from measured 1000-day deflection w_{1000} for 36 sets of bridge deflection records for average concrete properties, obtained using models CEB-*fib* (— · —), ACI-209 (——), RILEM-B3 (——), and RILEM-B3 model (— —) with terminal slope adjusted by $r = 1.6$.

Extrapolated Deflections of 36 Bridges [(deflection/span)% vs. time in days] ctd.

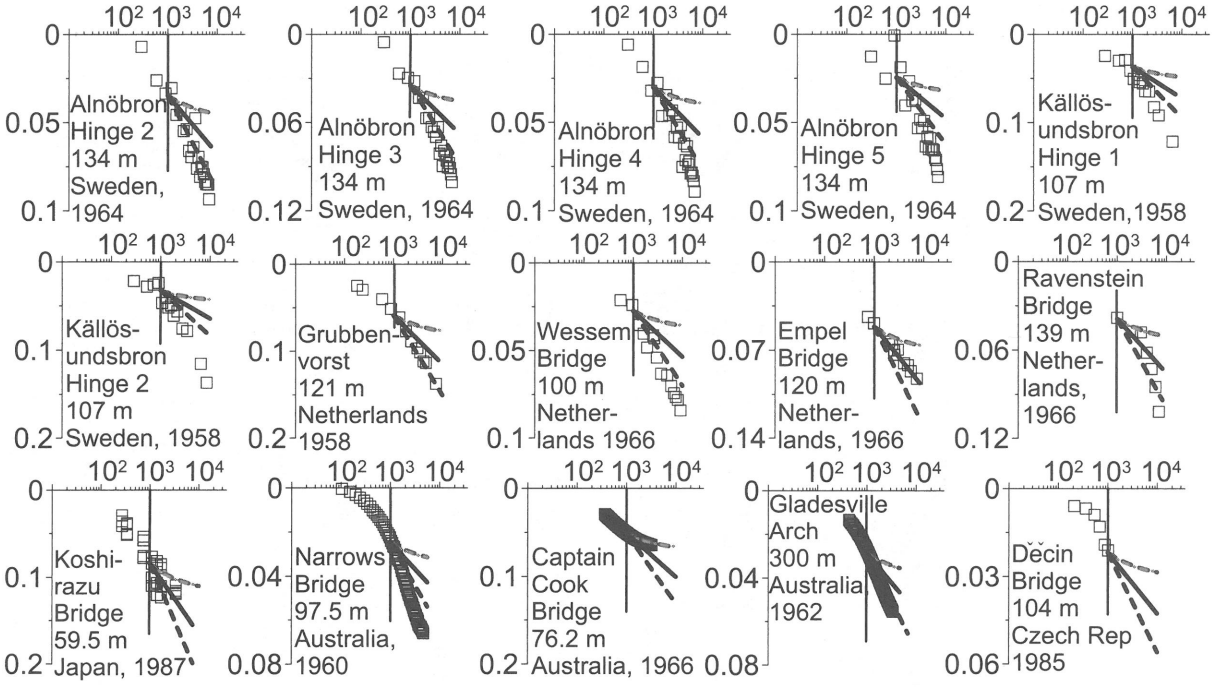

Figure 3 continued

2. Myth and reason in size effect

The size effect has been a contentious subject ever since the pioneering large beam tests of Kani in the 1960s [32], and the design codes have greatly lagged behind the theory. The 2010 *fib* Model Code Draft now proposes in Eqs. 7.3-18, 21, and 25 the beam shear model stemming from the work of Collins et al. in Toronto [33, 34, 35]. Although this model is a progress compared to the previous empirical one in the 1990 CEB Model Code [13], it is a dubious choice since there exists a better model, with a deeper and broader theoretical justification. This model, developed at Northwestern (Eq. 4 in [36, 37]), was unanimously endorsed by ACI Committee 446, Fracture Mechanics (Eq. 2 in [38]).

In comparison to the ACI-445F database of 398 tests of shear failure of RC beams (Fig. 4a, [36]), both models look about equally good (or equally bad), but this is deceptive. The quality of model cannot be judged because of a limited size range of the database, and because of a huge scatter band width when tests from different labs, made with different concretes, different steel ratios ρ and different shear spans a/h, are combined in one database. If extrapolated to real structure sizes larger than those in the database, the difference between the two models becomes significant.

One cannot validate a code equation solely by comparisons with a database that covers only a part of the size range of interest and has various kinds of statistical bias. A sound theoretical basis is required, too. But from the theoretical point of view, the procedure of derivation of the proposed *fib* Eqs. 7.3-18, 21, 25 is more a myth than logic. Briefly, note the following (and for a deeper critique, see pages 1892-1894 of [36]):

1) The average ultimate shear stress of the cross section is assumed to decrease with the beam depth (or size) h as $(1 + ch)^{-1}$ where c = constant. This kind of size effect means that the large size asymptote is proportional to h^{-1}, which is the Leonardo (da Vinci [39]) size effect law (contested by Galileo Galiei [40]). But this asymptote, which is also incorrectly exhibited by *fib* Eq. 7.3-40 for punching shear, is thermodynamically impossible. The strongest possible size effect on nominal strength is proportional to $h^{-1/2}$.
2) The model in *fib* Eqs. 7.3-18, 21, 25 was derived [33, 34] under the tacit hypothesis that the diagonal shear crack would open along its entire length simultaneously, as for a limit load in plasticity. But this is impossible in a quasibrittle material (the crack front actually propagates, and finite element simulations document that).
3) An additional tacit hypothesis in the derivation [33, 34] was that the cohesive stress transmitted across the diagonal shear crack would soften as $(1 + kw)^{-1}$ where w is the crack opening displacement and k = constant. This hypothesis, which is what led to $(1 + ch)^{-1}$, has not been justified. It conflicts, in fact, with the cohesive softening law generally used in concrete fracture community, which is a bilinear law with a steep initial decline and a long tail [41]. If the line of

reasoning in [33, 34] were accepted, this realistic cohesive softening law would lead to a very different size effect.

4) If, instead of $(1 + kw)^{-1}$, the cohesive stress across the diagonal shear cracks were assumed to soften as $(1 + kw)^{-1/2}$ (which would be less unrealistic because the softening tail would be relatively longer), the same (dubious) method of derivation [33, 34] of *fib* Eqs. 7.3-18, 21, 25 would indicate that the average ultimate shear stress of the cross section decreases with the beam depth h as $(1 + ch)^{-1/2}$, which is the (Bažant) Size Effect Law (SEL) [42], first proposed for beam shear in 1984 [43] and used in the recommendation unanimously adopted by ACI Committee 446, Fracture Mechanics.
5) The model in *fib* Eqs. 7.3-18, 21, 25 was derived [33] by incorporating the crack softening law $(1 + kw)^{-1}$ in the earlier 'Modified Compression Field Theory' (MCFT). This is, however, a stress-based (non-energetic) plasticity-type theory. The undeclared hypothesis in this derivation, which is almost true for small beam sizes (as in the laboratory), is that the concrete cracking remains distributed, non-localized, that the failure is almost simultaneous, non-propagating, and that the material strength is, at maximum load, almost mobilized along the entire failure surface. But this derivation is incorrect for large beam sizes beyond the laboratory scale, in which the cracking localizes, the failure propagates. This means that while, in one part of the failure surface and at maximum load, the peak stress point has already been passed and the stress has already softened below the material strength limit, in another part of the failure surface the material strength limit has not yet been reached at maximum load (Fig. 4). In other words, the material strength along the failure surface in large structures cannot get mobilized simultaneously (Fig. 4), but in small structures can. This aspect is best handled by considering the energy release rate, as in fracture mechanics [41] and in the derivation of SEL. However, the derivation of *fib* Eqs. 7.3-18, 21, 25 involves no energy-based consideration, as well as no fracture-related characteristic length, while the presence of a material characteristic length is in the mechanics community generally accepted as the ultimate cause of all non-statistical size effects.
6) The model in *fib* Eqs. 7.3-18, 21, 25 [33] may be applied to the diagonal crack initiation which, however, occurs long before the ultimate load is reached.
7) The implied assumption that the shear transmission across the developing diagonal crack controls the shear force capacity of the beam is an old, and false, myth. Detailed finite element analyses with an experimentally calibrated finite element fracture program [37] showed that the diagonal shear crack (Fig. 4) transmits 40% of the total shear force when the beam depth h is 0.3m, 17% when it is 2.0 m, and only 9% when it is 6.0 m. What controls the maximum load is the propagation of compression-shear crushing across the ligament above the diagonal crack tip (Fig. 4). And what explains the size effect is that, at maximum load, the compressive stress distribution across this ligament is in small beams nearly uniform, equal to concrete compression strength fcm,, whereas in large beams it is highly localized (Fig. 4). While one portion of the ligament in large

beams has not yet reached the concrete strength, another portion has already entered the post-peak regime and has softened to small stress (Fig. 8c,d [36]).

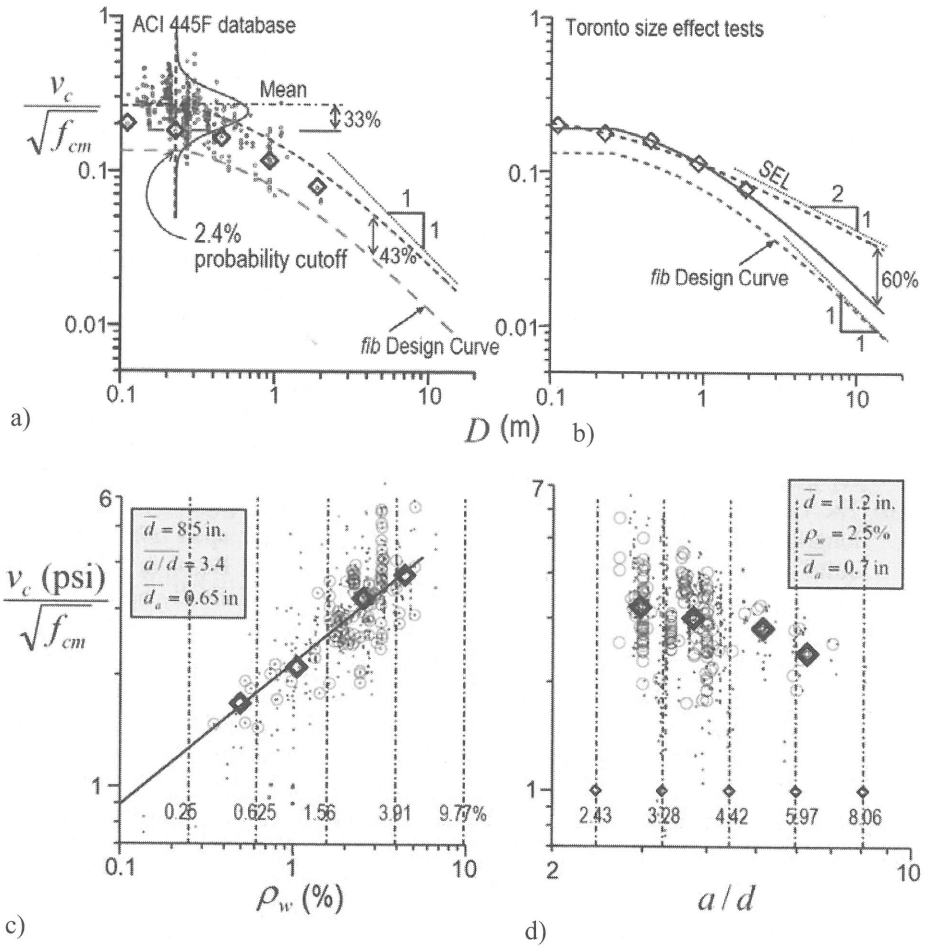

Fig. 4 a,b) Size effect curve for beam shear strength v_c based draft *fib* Eqs. 7.3-18, 21, 25 (long dashes), and the same curve shifted up by 43 % (in log-scale) to represent the mean fit (short dashes), a) compared to (biased and unfiltered) ACI-445F database, and b) to Toronto size effect tests made for one concrete, one beam shape (bold diamonds). c,d) trends of v_c dependence on longitudinal reinforcement ratio ρ_w and relative shear span a/h (where $d=h$), experimentally revealed by the centroids of database strips that were filtered so as to make other influencing variables the same in all the intervals (f_{cm} = mean cylindrical strength in psi (6895 Pa)).

8) The aggregate interlock stresses sketched in *fib* Fig. 7.3-4 may characterize the situation at diagonal crack initiation and, if the beam is small, partly also the situation at maximum load. But this traditional sketch, featured in old textbooks, is in the case of maximum load in large beams misleading because the stress along the diagonal crack does not get mobilized simultaneously along the entire crack length. Fig. 3e,f shows localized tensile and shear stress distribution along the diagonal crack and localized compressive stress distribution across the ligament above the tip of the diagonal crack, computed by a finite element program with the microplane model and crack band model for nonlocal damage [37].
9) The SEL [42] for structures reaching the maximum load only after the formation of a large crack has been validated for all kinds of quasibrittle failure of concrete structures, including anchors, beam torsion, slab punching, pipes and, in reduced-scale tests and in a slightly modified form, slender columns, and serves as standard fracture test basis. It has also been validated and widely accepted for all other quasibrittle materials, including sea ice, fiber composites, coarse-grained or toughened ceramics, wood, inhomogeneous rocks, stiff soils, bones, rigid foams, dry snow slabs, carton, etc. Why should then the size effect for shear of concrete beams be different?
10) The model in *fib* Eqs. 7.3-18, 21, 25 (as well as ACI) ignores the effects of longitudinal reinforcement ratio ρ and of relative shear span a/h, which are quite significant; see Fig. 3 c,d (and also Fig. 4c,d and Eq. 4 in [37]). The existing worldwide database of 398 tests (Fig. 3a) is statistically biased in that the means of ρ and of a/h in subsequent size intervals vary with the beam size (or depth) h. Vice versa, the mean of size h in subsequent intervals varies with ρ and a/h (Fig. 4c,d). To extract the trends, the database must be filtered. A computer program has been developed to filter the worldwide database by progressively deleting marginal points from the database such that the means of h and of a/d be very nearly the same in all the intervals, as shown by the values in Fig. 4c (and likewise in Fig. 4d) [44]. The data points deleted from the margins by the filtering program are shown in Fig. 4c as the tiny dots, and the data retained as the circles. Fig. 4c shows the centroids of the data remaining in each interval of ρ by the bold diamonds (and likewise Fig. 4d for the intervals of a/d. Fig. 4c documents that the beam shear strength v_c depends strongly on reinforcement ratio ρ (e.g., for $\rho > 3.9$ the v_c value is 2.9 times larger than it is for $\rho < 0.63$ if h and a/d are kept constant). Fig. 4d documents similarly that the dependence of v_c on a/d is significant, too. Both these effects are included in the beam shear equation in [38], calibrated by nonlinear regression, but are not revealed by the way of argument in MCFT. They should not be ignored in the future *fib* Model Code (as well as ACI Code).
11) Finally, it is not correct for *fib* (as well as ACI) to assume that minimum stirrups, or any stirrups, eliminate the size effect [45]. They merely mitigate it, pushing it into much larger beam sizes; see [46] and Fig. 5. Although the database with 183 data in Fig. 5 is too scattered to show a clear trend (mainly

because it combines many different concretes), the size effect trend is clearly revealed by computations with the crack band model [46] and is experimentally evidenced by the data of Bhal [47] for one and the same concrete, shown by bold diamonds in Fig. 5. In the presence of stirrups, the size effect can be ignored only for beam depths up to about 1 m, but for the depth of 6 m, typical, e.g., of the outriggers of modern super-tall buildings, the size effect reduces the shear capacity by roughly 40%, and for the depth of KB Bridge girder (14.2m) by roughly 50% [46]. As shown in Fig. 5, the failure probability is 10^{-6} for beam depth 0.3 m, as required, but increases to the unacceptable value of 10^{-3} for beam depth 6 m (the strength distribution is here assumed to be lognormal, rather than Gauss-Weibull, because the database compares many different concretes, which means that this is the strength probability when no tests for the given concrete have been made).

The simplest remedy to the size effect formulation in [14] would be to adopt the size effect equations adopted by ACI Committee 446, Fracture Mechanics [38], although they could be refined further.

There are other claims about the size effect, which are myth or fib (cf., e.g., [48]). They can be left aside.

3 Black holes in safety specifications

3.1 Black hole in probability distributions tails

In the mostly excellent chapters 4.5 and 4.6 on the safety formats [14], a glaring weakness is that all the probability density functions (pdf) of strength are tacitly assumed to be Gaussian (or normal). This is correct for ductile (or plastic) failures (because the Central Limit Theorem applies). But it is incorrect for brittle or quasi-brittle failures occurring at macro-fracture initiation from a small representative volume element (RVE) of material, which is what occurs in unreinforced structures (arch dams, foundation plinths, retaining walls, etc.), though not in most reinforced ones. For brittle failures, the pdf cannot be anything but Weibullian because the weakest link model for a chain with an infinite number of links [49] applies [50, 51]. It is well established that, for small sizes, the cracking remains distributed, which leads to a ductile (or quasi-plastic) failure, whereas for large sizes the cracking localizes, which leads to brittle failure. So it is logical to expect, and has been proven in various ways [50, 51, 52], that the pdf must gradually change from Gaussian to Weibullian as the structure size increases. And that is where the black hole resides.

It is generally agreed [53, 54, 55] that engineering structures must be designed for failure probability $P_f < 10^{-6}$, and so the tail of the pdf of strength needs to be known within the range 10^{-5}—10^{-6} (which is what matters for the convolution integral with the pdf of load). Now, for the Weibull pdf, the distance from the mean to the tail point of 10^{-6} is

almost twice as large, in terms of standard deviations, as it is for the Gaussian pdf (Fig. 4), and this has a big effect on the required (partial) safety factor. But such a far out-tail is like a black hole—it is not directly observable by histogram testing (since $>10^8$ structure test repetitions would be needed!). Yet, like a black hole, the tail can be observed indirectly — through the size effect (of type 1 [56]), which is dominated by the tail [51].

This scaling behavior has recently been researched and experimentally demonstrated in theoretical literature [50, 51, 52], but it will take some effort to build it into the system of partial safety factors for concrete structures. Until this is done, it is an illusion to think that the failure probability could be calculated for large concrete structures failing at macro-crack initiation.

Another problem with a black hole in the tail arises from the use of lognormal distribution in Eq. 4.5-9b [14] for the updated design value x_d of structural resistance X .The lognormal distribution is appropriate to characterize the statistical variability arising when different concretes are considered [44] (Fig. 5). This variability is huge and overrides the statistical variability of one concrete *per se*. However, to characterize the randomness of resistance of a structure made from one and the same concrete, or the material strength of one and the same concrete, the lognormal distribution is incorrect, physically inconceivable.

In ductile failure, the resistance X is a sum of weighted random contributions from many simultaneously failing material elements along the failure surface, with weights that can be determined, e.g., by a finite element code. Hence, according to the Central Limit Theorem, the structure strength distribution must be Gaussian — except, of course, the tail, including the far-left tail reaching into negative values, which is always beyond the range of validity of the Gaussian pdf (note that even the sum of n positive independent identically distributed random variables, which can never be negative, converges to the Gaussian distribution as $n\rightarrow\infty$).

The only way a lognormal distribution for one given material (i.e., one concrete) could physically arise is if the failure were a product, rather than a sum, of the random strength contributions of the material elements along the failure surface [52]. But such a product, which is implied by the lognormal distribution, is of course physically inconceivable, for both structure strength and material strength. Thus, provided that one given concrete is considered, the lognormal distribution in fib Eq. 4.5-9a should be replaced by the Gaussian pdf if the failure is ductile, by the Gauss-Weibull graft [52, 51] (which corresponds to a finite weakest-link model) if it is quasibrittle, and by the Weibull pdf (which corresponds to an infinite weakest-link model) if it is perfectly brittle.

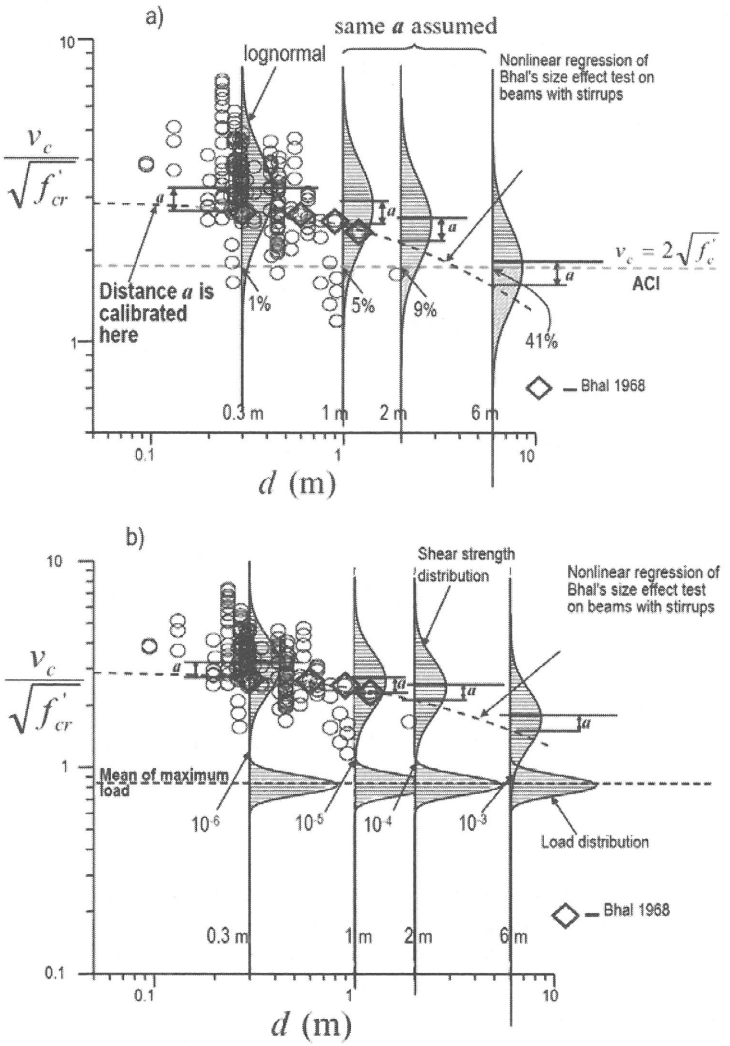

Fig. 5 Size effect on shear strength of RC beams with stirrups, compared to the database of 183 tests [46] for many different concretes, and lognormal strength distributions assumed to be, for all the sizes d (d=h), the same as in the small size interval with many data. The bold diamonds represent the tests of Bhal on one and the same concrete a) The increasing probability cutoff indicates the decrease of safety margin with increasing size. b) Comparison with typical maximum design load distributions, and failure probabilities for various sizes obtained by convolution with strength distribution according to Freudenthal reliability integral.

Note also that since the lognormal distribution has the opposite skewness than the Weibull distribution, it represents, for the variability of strength of one given concrete, the worst possible guess [52] for someone who is bothered by the infinite Gaussian tail reaching into negative values. The difference in the safety factor corresponding to the tail at Pf =10-6 is huge (Fig. 6).

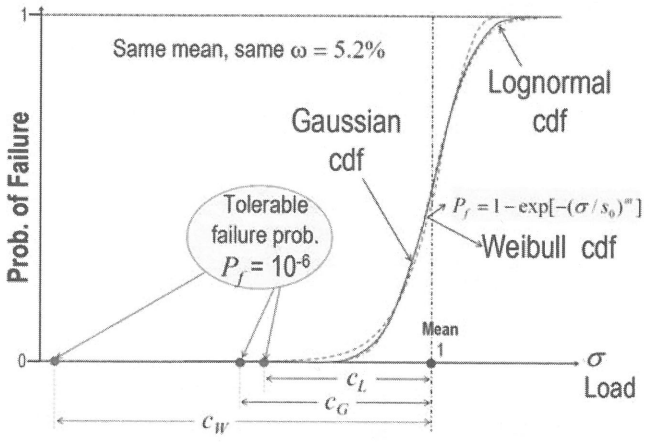

Fig. 6 Gaussian, Weibull, and Lognormal cumulative probability density functions with the same mean, equal to 1, and the same typical coefficient of variation. Note the huge differences among the distances c_G, c_W *and* c_L from the mean to the tail point with probability 10^{-6} (a point that matters for safe design).

The problem of a black hole in the tail extends to the use of reliability index β in *fib* subclause 3.2.5. That index, too, is predicated on the Gaussian distribution and thus cannot be applied if the structural failure is not ductile, lacking a long plastic plateau on the load-deflection diagram. This limitation should be kept in mind.

3.2 Black holes in design formulas set at the margin of data

Another aspect that confounds the calculation of failure probability on the basis of design formulas is the presence of the so-called covert safety factors [57]. In the *fib* Model Code Draft (as well as in ACI code), for example, the design equation (*fib* Eq. 7.3-8) for beam shear has not been set so as to represent the mean trend of the data, i.e., the regression curve. Rather, it has been set at about 43% below the regression curve. Because this fact is kept invisible in the code, the code formula is often taken as the mean prediction, which obviously leads to wrong estimates of failure probability.

Again, this is a sort of a black hole, though an easier one. It would suffice for the designer to plot the *fib* Eq. 7.3-8 against the database, carry out the nonlinear regression, and determine the probability cut-off for the offset of the design equation from the regression curve in the interval of interest. However, this is not what the designers are expected to do. The code should make it easy: Declare in the code the probability cutoff of the recommended design equation, the coefficient of variation, and the type of distribution. Otherwise all the failure probability estimates are meaningless.

This black hole, as well as that in tails, can, in principle, be avoided if the failure probability is calculated by a stochastic nonlocal (fracture-based) finite element code into which the Gauss-Weibull transition of pdf is incorporated. But this is a complex task, still in the research realm, and a practical way to deal with these black holes in the pdf tails does not yet exist.

3.3 False size effect hidden in excessive partial safety factor imposed on self-weight

For permanent actions, which include the self-weight, Section 4.5.2 of the *fib* Model Code Draft specifies the load factors of 1.05 – 1.1 in Table 4.5-4, 1.35 in section 4.5-5 for the case of "non-particular" actions, not involving geotechnical actions, and either 1.35 or 0.85 – 1.35 in Table 4.5-6 for alternative combination. Although the application is not completely clear from this Draft, it is clear, upon rigorous appraisal, that 1.1, and especially 1.35, are irrational. The same could be said of the ACI Standard 318, which specifies for dead load, including the self-weight, the factor of 1.4 when acting alone and 1.2 when in combination.

In a small bridge, the self-weight may represent only a few percent of the total load. But in a large bridge, more than 95% of the total load can be the self-weight of concrete. Errors larger than about 3% in the weight of concrete and reinforcement are inconceivable (except as carelessness or sabotage). Thus the factors of 1.1 and 1.35 represent a penalty on large structures, which represents a hidden size effect [58]. This size effect is invisible to the designer, like a black hole.

However, the self-weight factor is not a rational way to introduce the size effect. The shape of the size effect curve implied by these factors is incorrect [58]. Besides, prestressed structures, or structures made with high strength concrete, are lighter than the unprestressed ones or those made with normal strength concretes, and thus the size effect hidden in excessive self-weight factor is weaker, yet in reality the size effect is stronger because such structures are more brittle. For large cable-stayed bridges, this hidden size effect also works the wrong way.

4. Closing comment

Although a perfect design code is unattainable, and too much perfection would make the code too complex to use, some corrections outlined here are simple and easy to implement. They would improve the *fib* Model Code Draft substantially.

Financial supports from the U.S. Department of Transportation through Grant 23120 from the Infrastructure Technology Institute of Northwestern University, and the US National Science Grant CMS-0556323 are gratefully appreciated. Thanks are due to Y. Watanabe, G. Klein, V. Šmilauer, L. Vráblík, M. Lepš, J. Vítek, M. Zich, J. Navrátil, M. Jirásek, B. Teplý, V. Červenka, D. Novák and M. Vořechovský for valuable help in obtaining various data and for many helpful comments.

References

[1] Bažant, Z.P., Yu, Q., Li, G.-H., Klein, G.J., and Křístek, V. (2010), "Excessive deflections of record-span prestressed box girder: Lessons learned from the collapse of the Koror-Babeldaob Bridge in Palau." *ACI Concrete International* 32 (6), June, 44-52.

[2] Bažant, Z.P., and Yu. Q. (2011). "Excessive Long-Time Deflections of Prestressed Box Girders: I.Record-Span Bridge in Palau and Other Paradigms, II. Numerical Analysis and Lessons Learned." *ASCE J. of Engrg. Mechanics*, in press.

[3] Berger/ABAM Engineers Inc. (1995b). "Koror-Babeldaob Bridge Repair Project Report on Evaluation of VECP," presented by Black Construction Corporation, June. *KB Bridge modifications and repairs.*

[4] Berger/ABAM Engineers Inc. (1995a). "Koror-Babeldaob Bridge modifications and repairs", October.

[5] Japan International Cooperation Agency. (1990) "Present Condition Survey of the Koror-Babelthuap Bridge", Feburary.

[6] Shawwaf, Khaled (Dir., Dywidag Systems International USA, Bollingbrook, Illinois; former structural analyst on KB bridge design team), *Private communication*, September 18, 2008, Chicago.

[7] Zelinski, Raymond (former Bridge Engineer, Caltrans, California), *Private communication*, Dec. 12, 2010.

[8] Bažant, Z.P. and Baweja, S. (1995). "Creep and shrinkage prediction model for analysis and design of concrete structures: Model B3" (RILEM Recommendation) *Materials and Structures* 28, pp. 357--367 (Errata, Vol. 29, p. 126).

[9] Bažant, Z.P. and Baweja, S. (2000). "Creep and shrinkage prediction model for analysis and design of concrete structures: Model B3." *Adam Neville Symposium: Creep and Shrinkage---Structural Design Effects*, ACI SP--194, A. Al-Manaseer, ed., pp. 1--83 (update of 1995 RILEM Recommendation).

[10] Brooks, J.J., (2005) "30-year creep and shrinkage of concrete," *Magazine of concrete research* 57, pg. 545-556.

[11] ACI Committee 209 (1972, 2008) "Prediction of creep, shrinkage and temperature effects in concrete structures" *ACI-SP27, Designing for Effects of Creep, Shrinkage and Temperature*, Detroit, pp. 51—93 (reapproved 2008).

[12] ACI Committee 209 (2008). "Guide for Modeling and Calculating Shrinkage and Creep in Hardened Concrete." *ACI Report 209*.2R-08, Farmington Hills.

[13] CEB-FIP Model Code 1990. Model Code for Concrete Structures. Thomas Telford Services Ltd., London, Great Britain; also published by Committee euro-international du béton (CEB), Bulletins d'Information No. 213 and 214, Lausanne, Switzerland.

[14] Draft of fib Model Code 2010. "Fédération internationale de béton (fib)." Lausanne.

[15] FIB (1999). "Structural Concrete: Textbook on Behaviour, Design and Performance, Updated Knowledge of the CEB/FIP Model Code 1990." Bulletin No. 2, Fédération internationale du béton (FIB), Lausanne, Vol. 1, pp. 35--52.

[16] Gardner, N.J., and Lockman, M.J. (2001) "Design provisions for drying and creep of normal-strength concrete." *ACI Materials Journal*, 98 (2): 159-167.

[17] "Standard Specifications for Design and Construction of Concrete Structures. Part I, Design." Japan Soc. of Civil Engrs. (JSCE), 1996 (in Japanese).

[18] "Specifications for Highway Bridges with Commentary. Part III. Concrete." Japan Road Association (JRA), 2002 (in Japanese).

[19] Vítek, J.L., (1997) "Long-Term Deflections of Large Prestressed Concrete Bridges," CEB Bulletin d'Information No. 235, "Serviceability Models" Behaviour and Modeling in Serviceability Limit States Including Repeated and Sustained Load, CEB, Lousanne, pp. 215-227 and 245-265.

[20] Burdet, O., Muttoni, A., (2006) "Evaluation of existing measurement systems for the long-term monitoring of bridge deflections," Confederation Suisse, Dec.

[21] Fernie, G. N., Leslie, J. A., (1975) "Vertical and Longitudinal Deflections of Major Prestressed Concrete Bridges," Institution of Engineers, Australia n7516, *Symposium of Serv. Of Concrete*, Melbourne, Aug 19.

[22] Pfeil, W., (1981) "Twelve Years Monitoring of Long Span Prestressed Concrete Bridge," *Concrete International.* Vol . 3 No. 8, pg. 79-84, Aug. 1.

[23] Manjure, P. Y., (2001-2002) "Rehabilitation/Strengthening of Zuari Bridge on NH-15 in Goa," Paper No.490, Indian Roads Congress, pp. 471.

[24] Bažant, Z.P., Carreira, D., and Walser, A. (1975). "Creep and shrinkage in reactor containment shells." *Jour. Struct. Div.*, Am. Soc. Civil Engrs., 101, 2117--2131.

[25] Bažant, Z.P., and Li, Guang-Hua (2008). "Comprehensive database on concrete creep and shrinkage." *ACI Materials Journal.* 106 (6, Nov.-Dec.), 635--638.

[26] Bažant, Z.P. and Li, G.-H. (2008). "Unbiased Statistical Comparison of Creep and Shrinkage Prediction Models." *ACI Materials Journal.* 105 (6): 610-621.

[27] Bažant, Z.P., Hubler, M.H., Yu, Q. (2010) "Pervasiveness of Excessive Deflections of Segmental Bridges: Wake-Up Cal for Creepl" Structural Egrg.Report, Northwestern University, submitted to ACI J.

[28] RILEM Committee TC-69 (1988). "State of the art in mathematical modeling of creep and shrinkage of concrete" in *Mathematical Modeling of Creep and Shrinkage of Concrete.*, ed. by Z.P. Bažant, J. Wiley, Chichester and New York, 1988, 57--215.

[29] Bažant, Z.P. (2000) "Criteria for Rational Prediction of Creep and Shrinkage of Concrete." *Adam Neville Symposium: Creep and Shrinkage - Structural Design Effects*, ACI SP-194, A. Al-Manaseer, ed., Am. Concrete Institute, Farmington Hills, Michigan, pg. 237-260.

[30] Bažant, Z.P., and Huet, C. (1999). "Thermodynamic functions for ageing viscoelasticity: integral form without internal variables." *Int. J. of Solids and Structures*. 36, 3993--4016.

[31] Bažant, Z.P. and Yu, Q. (2011) "Constitutive Equation for Stress Relaxation in Prestressing Steel at Varying Strain," submitted.

[32] Kani, G.N.J. (1967). "How safe are our large reinforced concrete beams?" *ACI J.*, 58(5), 591--610.

[33] Vecchio, F.J., and Collins, M.P. (1986). "The modified compression field theory for reinforced concrete elements subjected to shear." *ACI J.. Proc.* 83 (2), 219--231.

[34] Collins, M.P., and Mitchell, D. (1991). *Prestressed concrete structures.* Prentice Hall, Englewood Cliffs, New Jersey 1991 (section 7.10).

[35] Bentz, E.C. and Collins, M.P. (2006) "Development of the 2004 Canadian Standards Association (CSA) A23.3 shear provisions for reinforced concrete." *Canadian Journal of Civil Engineering*. 33 (5) pg. 521-534.

[36] Bažant, Z.P., and Yu, Q. (2005). "Designing against size effect on shear strength of reinforced concrete beams without stirrups: I. Formulation" *ASCE J. of Structural Engineering.* 131 (12), 1877--1885.

[37] Bažant, Z. P. and Yu, Q. (2005) "Designing Against Size Effect on Shear Strength of Reinforced Concrete Beams without Stirrups: II. Verification and Calibration." *ASCE J. of Structural Engineering.* 131 (12) 1886-1897.

[38] Bažant, Z. P., Yu, Q., Gerstle, W., Hanson, J. and Ju, J.W. (2007) "Justification of ACI 446 Proposal for Updating ACI Code Provisions for Shear Design of Reinforced Concrete Beams." *ACI Structural Journal.* 104 (5) pg. 601-610 (Errata, Nov.-Dec., p. 767).

[39] da Vinci, L. (1500s) – see *The Notebooks of Leonardo da Vinci.* (1945), Edward McCurdy, London (p. 546); and *Les Manuscrits de Léonard de Vinci*, transl. in French by C. Ravaisson-Mollien, Institut de France (1881-91), Vol. 3.

[40] Galileo Galilei Linceo (1638) *Discorsi i Demostrazioni Matematiche intorno à due Nuove Scienze*, Elsevirii, Leiden. (English transl. by T. Weston, London (1730), pp. 178--181)

[41] Bažant, Z.P., and Planas, J. (1998). *Fracture and Size Effect in Concrete and Other Quasibrittle Materials*. CRC Press, Boca Raton and London.

[42] Bažant, Z.P. (1984). "Size effect in blunt fracture: Concrete, rock, metal." *J. of Engrg. Mechanics*, ASCE, 110 (4), 518–535.

[43] Bažant, Z.P., and Kim, Jenn-Keun (1984). "Size effect in shear failure of longitudinally reinforced beams." *Am. Concrete Institute Journal*, 81, 456–468; Disc. & Closure 82 (1985), 579–583.

[44] Bažant, Z.P. and Yu, Q. (2009) "Does Strength Test Satisfying Code Requirement for Nominal Strength Justify Ignoring Size Effect in Shear?" *ACI Structural Journal.* 106 (1) pg. 14-19.

[45] Bažant, Z.P., and Sun, H-H. (1987). "Size effect in diagonal shear failure: Influence of aggregate size and stirrups." *ACI Materials Journal.* 84 (4), 259-272.

[46] Bažant, Z.P., and Yu, Q. (2011). "Can Stirrups Suppress Size Effect on Shear Strength of RC Beams?" *ASCE J. of Structural Engineering*, in press

[47] Bhal, N.S. (1968). *Űber den Einfluss der Balkenhöhe auf Schubtragfähighkeit von einfeldrigen Stalbetonbalken mit und ohne Schubbewehrung.* Dissertation, Universität Stuttgart.

[48] Bažant, Z.P., and Yavari, A. (2005). "Is the cause of size effect on structural strength fractal or energetic-statistical?" *Engrg. Fracture Mechanics*. 72, 1-31.

[49] Weibull, W. (1939). "A statistical theory of the strength of materials." *Proc. Royal Swedish Academy of Eng. Sci.*151, 1-45.

[50] Le, J.-L., Bažant, Z.P., and Bazant, M.Z. (2011). "Unified Nano-Mechanics Based Probabilistic Theory of Quasibrittle and Brittle Structures: I. Strength, Static Crack Growth, Lifetime and Scaling." *J. of the Mechanics and Physics of Solids.* in press.

[51] Bažant, Z.P., Le, J.-L., and Bazant, M.Z. (2009), "Scaling of strength and lifetime probability distributions of quasibrittle structures based on atomistic fracture mechanics," *Proc. of the National Academy of Sciences.* 106 (28), 11484--11489.

[52] Bažant, Z. P., and Pang, S.-D. (2007) "Activation energy based extreme value statistics and size effect in brittle and quasibrittle fracture." *J. Mech. Phys. Solids.* 55, pp. 91-134.

[53] Duckett, K. (2005). "Risk analysis and the acceptable probability of failure." *The Structural Engineering.* 83 (15), pp 25-26.

[54] NKB (Nordic Committee for Building Structures) (1978). *Recommendation for loading and safety regulations for structural design.* NKB Report, No. 36.

[55] Melchers, R. E. (1987) *Structural Reliability, Analysis & Prediction.* Wiley, New York.

[56] Bažant, Z.P. (2004). "Scaling theory for quasibrittle structural failure." *Proc., National Academy of Sciences.* 101 (37), 13400--13407.

[57] Bažant, Z.P., and Yu, Q. (2003), "Reliability, brittleness and fringe formulas in concrete design codes," Infrastructure Technology Institute Report No. 03-12/A466r, Northwestern University; also *J. of Structural Engrg. ASCE*, submitted.

[58] Bažant, Z.P., and Frangopol, D.M. (2002). "Size effect hidden in excessive dead load factor." *J. of Structural Engrg. ASCE* 128 (1), 80–86.